Lithuanian Journal of Physics
Vol. **64**, No. 1, pp. 48–57 (2024)
ISSN 1648-8504 eISSN 2424-3647
DOI: https://doi.org/10.3952/physics.2024.64.1.5

NUMERICAL SIMULATION OF PROTON BACKSCATTERING SPECTRA IN GEANT4 TOOLKIT

D. Lingis, M. Gaspariūnas, V. Kovalevskij, A. Plukis, and V. Remeikis

Center for Physical Sciences and Technology, Savanorių 231, 02300 Vilnius, Lithuania
Email: danielius.lingis@ftmc.lt

Received 15 May 2023; accepted 3 October 2023

Rutherford backscattering spectroscopy (RBS) is a widely used technique for the atomic-scale analysis of sample composition, lattice displacement and impurity profiling. RBS is based on the elastic scattering of incident charged particles by target nuclei and the subsequent detection of scattered particles. The interpretation of RBS spectra, however, poses challenges due to overlapping peaks, corresponding to scattering from different atomic species, and uncertainties from energy loss, scattering geometry and detector response. To address this, an open source simulation model based on the versatile GEANT4 simulation toolkit has been developed. The flexibility of the open source enables users to tailor the model to its specific requirements, such as the use of specific particle stopping powers, cross-sections, and physics processes. This work presents the results of the comparison between the experimental and simulated backscattering spectra in crystalline silicon, silicon carbide and silicon dioxide samples by 1–2.5 MeV energy protons, obtained in random orientation conditions. The results demonstrate the capability of the model to accurately simulate backscattering spectra in both amorphous materials and single crystals. The overall agreement between the simulated and experimental results is highly promising for future development and use in the interpretation and simulation of RBS spectra.

Keywords: Rutherford backscattering, GEANT4 simulations, backscattering spectra, protons
PACS: 82.80.Yc, 25.40.Cm

1. Introduction

Elastic backscattering spectroscopy (also known as Rutherford backscattering spectroscopy, RBS) is a widely used technique for the analysis of sample composition [1], lattice displacement [2], impurity profiling [3] and other studies at the atomic scale. As long as the particle flux and fluence are not inducing a significant displacement damage, the method offers a non-destructive and highly sensitive approach to the study of solid surfaces. The RBS technique is based on the phenomenon of the elastic scattering of incident charged particles by target nuclei and the subsequent detection of scattered particles outside the sample. By measuring the energy and yield of backscattered particles, the information about the sample composition, profile, layer structure, etc. can be retrieved. However, the interpretation of the spectra is a complex task due to several challenges that are inherent to this method. Firstly, in multi-layered and/or multi-elemental samples multiple overlapping peaks can occur from different scattering events of specific atomic species. Additionally, the intensity and shape of these peaks are significantly influenced by incident particle energy, scattering geometry, target compositions, etc. Finally, uncertainties of the spectra may be introduced by energy loss straggling [4], multiple scattering [5] and detector response [6] factors. Thus, the attribution of peaks to specific atom species and the determination of an elemental composition as well as the thickness of layers or profiles is a complex task that is challenging without the use of specialized spectra simulation or fitting tools. There are several simulation tools developed for this precise task, such as RBX [7], CORTEO [8], DEPTH [9], SIMNRA [10], IBA DataFurnace [11]

and others. However, these tools are either an outdated or a closed source, which limits versatility of these tools in specific cases where specific particle stopping powers or cross-sections are needed to use. An alternative open source backscattering spectra simulation model [12] has been recently developed which allows these drawbacks to be avoided. The model is based on a versatile open source simulation toolkit GEANT4 [13] that is constantly being developed with the addition of new physics processes, reaction cross-sections, stopping power libraries and others. The work presented here shows the comparison of the experimental and simulated backscattering spectra of protons in silicon, silicon carbide and silicon dioxide samples in the energy range 1–2.5 MeV.

2. Methodology

The simulation of particle trajectory in GEANT4 consists of steps, and the simulation of backscattering spectra involves evaluating the differential cross-section, yield, and final energy distribution at each such step position. The differential Rutherford scattering cross-section in the centre of mass (CM) reference frame is obtained from Ref. [14]:

$$\left(\frac{\mathrm{d}\sigma}{\mathrm{d}\Omega}\right)_{\mathrm{CM}} = \left(\frac{z_1 z_2 e^2}{16\pi\varepsilon_0 E_{\mathrm{CM}}}\right)^2 \frac{1}{\sin^4\left({}^{\theta_{\mathrm{CM}}}/_2\right)}. \qquad (1)$$

Here ε_0 is the vacuum permittivity, Ω is the solid angle, Z_1 and Z_2 are the charge numbers of the projectile and the target atom, respectively, and E_{CM} is the particle kinetic energy in the CM reference frame. The pure Rutherford cross-section often deviates from the experimental one [15] and modifications need to be taken into account. The low energy corrections of the cross-section are based on the Andersen shielding factor [16]. The differential cross-section is then modified by high energy corrections based on the ratio of the non-Rutherford to Rutherford cross-sections (RTR) factors in the resonant shapes of the cross-sections. The RTR values were obtained by using a SigmaCalc2.0 calculator [17]. The intensity or yield of backscattering is obtained by multiplying the differential cross-section by the detector solid angle and the atom density of the material (or element for multi-elemental targets) at the current step position. After calculating the yield of backscattering, the final energy of the outgoing particle is determined. To accomplish this, the distance between the backscattering depth and the surface of the sample is divided into 20 equally sized blocks. Within each block, the energy loss and energy loss straggling (both nuclear and electronic, refer to Ref. [12] for details) are integrated, utilizing the stopping powers specific to the amorphous material. The width of final energy distribution is determined by taking the square root of the sum of squared detector energy resolution and total energy loss straggling. A total of 200 energy points are generated, spanning from –20% to +20% of the final particle energy, based on the probability density function of Gaussian distribution. Each point is assigned a weight corresponding to the sum of probabilities for its energy value, and then incorporated into a histogram. The cumulative sum of all Gaussian distributions constitutes the final backscattering spectra.

The backscattering spectra obtained from the experiments were converted into a digital format by utilizing the WebPlotDigitizer 4.6 free application [18], based on Refs. [19–23]. The experimental amorphous spectra were obtained from crystal samples by setting the incident beam further from the channelling axis and then rotating the sample or beam while measuring, thus always measuring in a random (or rather a constantly changing) orientation. Although the materials are not amorphous, the random orientation technique is often used to obtain the spectra that are close to amorphous sample spectra. A summary of the materials and experimental conditions employed in this study can be found in Table 1. In the cases where the experimental curves were originally presented with channel numbers as the horizontal axis, a conversion from the channel number to energy was carried out. That conversion was accomplished using the SIMNRA toolkit [10]. During the simulations, the beam was configured to be monoenergetic and circular in shape. The experimental and simulated spectra were normalized to the total integrals of the corresponding curves.

The theoretical backscattering cross-sections for the atoms investigated in this study within an energy range of 0.25–3 MeV are illustrated in Fig. 1. These cross-sections encompass all the necessary corrections, including both high and low energy effects. Within the simulated energy range, the O-16 cross-section exhibits a relatively smooth behaviour with only a single dip at approximately 2.66 MeV.

Table 1. Experimental conditions.

Material	Detection angle, °	Detector energy resolution, keV	Beam energy, MeV	Material density in simulations, g/cm^3	Reference
Silicon	160	16	1.95–2.50	2.33	[19]
	170	8	1.50–2.15		[20]
	160	18	2.20–2.35		[21]
SiC	170	8	1.50–1.70	3.16	[22]
SiO_2	170	8	1.60–1.80	2.32	[23]

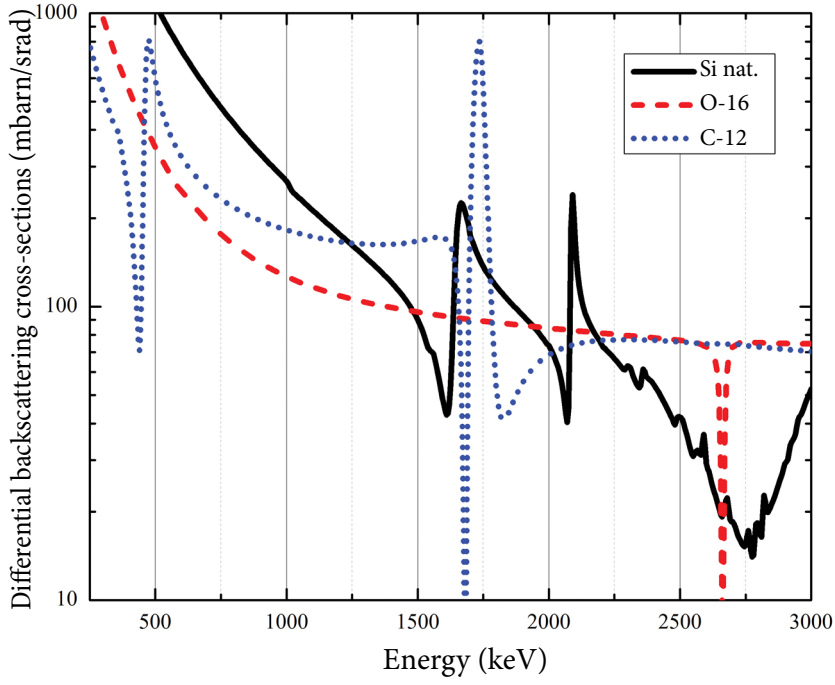

Fig. 1. The simulated differential backscattering cross-sections at 160° backscattering angle for natural composition silicon, O-16 and C-12 atoms, obtained by the GEANT4 RBS model.

In contrast, the backscattering cross-sections for C-12 and silicon atoms display resonant peaks: (a) at 0.48 and 1.73 MeV for C-12; (b) at 1.66 and 2.09 MeV for silicon atoms.

3. Results

3.1. RBS from Si sample

The comparison of the theoretical and experimental spectra for silicon was made using three separate experimental setups, with details described in Refs. [19–21]. The comparison of experimental and simulated spectra, obtained in the energy range 1.9–2.5 MeV at a backscattering angle of 160° shows a good agreement of the energy positions of the peaks (see Fig. 2). The overall shape of the simulated spectra is in good agreement with the experimental ones and the surface region (high energy side) is simulated correctly. In most cases, the simulated lower energy plateau regions match the experimental curves. However, the experimentally observed resonant peaks have less intensity compared to the simulated ones. One of the main reasons for this is the limitation of the accuracy of the theoretical cross-section. That limitation was previously observed and evaluated with the current RBS model [12]. Moreover, multiple and plural particle scattering processes are known to induce higher intensity in the low-energy region [5]. Another factor that might contribute to additional energy spread is the sample rotation. Due to the sample rotation around the beam axis, the distance between the backscattering depth and the surface of the detector fluctuates, resulting in additional

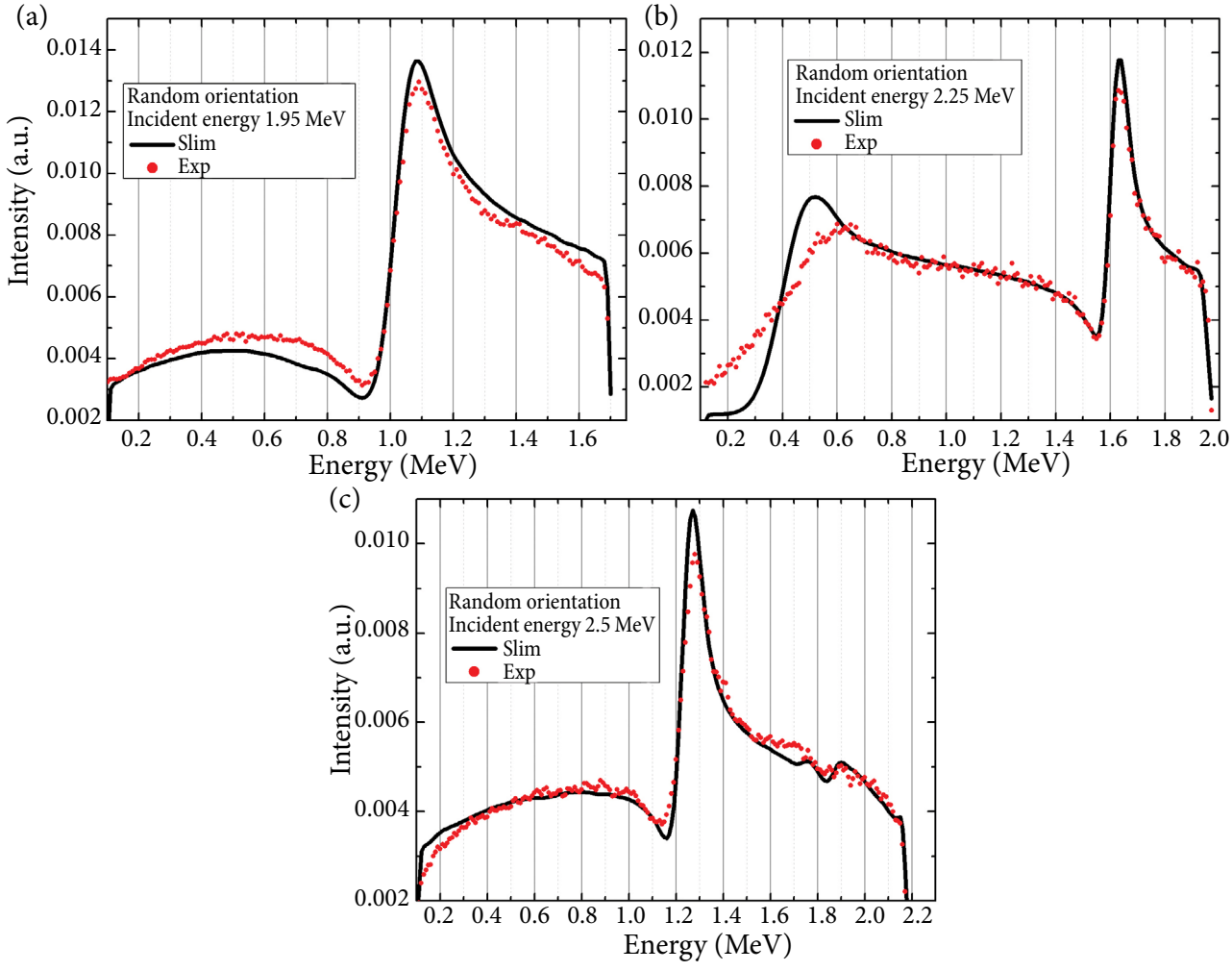

Fig. 2. Experimental and simulated backscattering spectra induced by 1.95 MeV (a), 2.25 MeV (b) and 2.5 MeV (c) protons incident on the crystalline Si sample under random orientation conditions. Experimental data digitized from Ref. [19].

energy spread. The combined effect of these factors can cause a mismatch between the experimental and simulated spectra.

The case of 1.95 MeV shows a moderate agreement between the experimental and simulated curves. The energy positions of the resonant peaks are simulated accurately; however, there is a clear mismatch in the intensity between the experimental and simulated data. The simulated curve exhibits a higher intensity in the high-energy region (1.0–1.7 MeV), while a significantly reduced intensity is observed after the resonant peak (0.1–0.9 MeV) compared to the experimental curve. For the case of 2.25 MeV, the experimental and simulated spectra agree very well within an energy interval of 0.6–2.0 MeV. However, significant differences are observed in the higher simulated intensity and sharpness of the resonant peak (~1.61 MeV) as well as the low-energy region (<0.6 MeV), where the intensity of the experimental spectra linearly decreases. In this latter case, the shape of the experimental spectrum does not follow the shape of the resonance cross-section at 1.67 MeV (see Fig. 1). On the other hand, the simulated curve shows an increase and a sharp decrease in intensity. Similarly, the 2.5 MeV case shows agreement between the experimental and simulated spectra, similar to the 2.25 MeV case. The simulated resonant peak (~1.27 MeV) has more intensity and sharpness when compared to the experimental spectrum.

Another comparison between the experimental and simulated backscattering spectra was made for 1.5 and 2.15 MeV protons, backscattered at an angle of 170° from the pure silicon crystal, with experimental data from Ref. [20]. In both cases, the match is almost perfect (see Fig. 3). The former

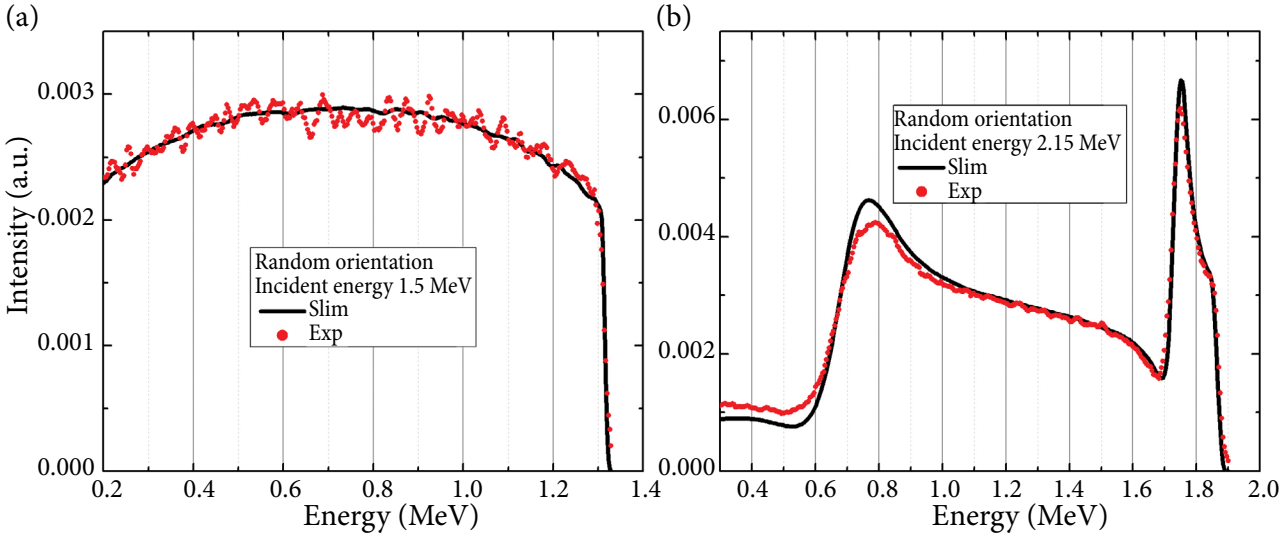

Fig. 3. Experimental and simulated backscattering spectra induced by using 1.5 MeV (a) and 2.15 MeV (b) protons incident on the crystalline Si sample under random orientation conditions. Experimental data digitized from Ref. [20].

shows a perfect agreement with the experimental spectrum as no resonant peaks are present. In the latter case, the intensity of the simulated spectrum of both resonant curves at 1.75 and 0.78 MeV shows a higher intensity when compared to that of the experimental spectrum; however, the shape of the curve is a close match to the experimental curve. In this case, the simulated low energy resonant peak is a closer match to the experimental peak when compared to the 2.25 MeV spectrum (see Fig. 2).

The final comparison of proton backscattering spectra from the pure silicon crystal was performed for 2.2–2.35 MeV protons at an angle of 160°, with experimental data digitized from Ref. [21]. When 2.2 MeV protons are simulated, the intensity of both resonant curves (at 1.7 and 0.65 MeV) is higher in the simulated case when compared to the experimental spectrum (see Fig. 4(a)). The major difference appears in the low energy region (0.2–0.8 MeV), where the simulated curve has more intensity than the experimental

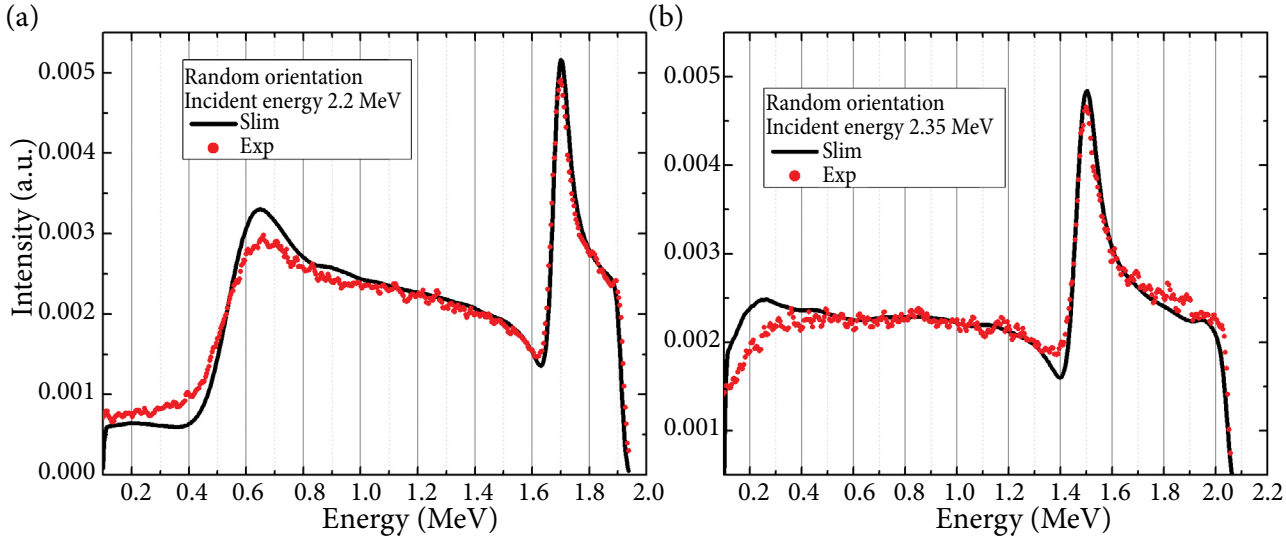

Fig. 4. Experimental and simulated backscattering spectra induced by 2.2 MeV (a) and 2.35 MeV (b) protons incident on the crystalline Si sample under random orientation conditions. Experimental results digitized from Ref. [21].

one. The 2.35 MeV case also shows a similar level of agreement between the experimental and the simulated spectra – the main resonant peak (at 1.5 MeV) and the low energy region (0.2–0.5 MeV) have a higher intensity in the simulated case when compared to the experimental spectrum (see Fig. 4(b)). One additional difference observed in this energy case for the experimental spectrum is the lack of cross-section dip after the resonant peak (at 1.4 MeV), which is clearly observed in the simulated spectrum. This might be due to the digitization error.

For 2.15–2.25 MeV proton induced backscattering spectra of several silicon samples, a distinct difference can be observed in the lower energy resonant peaks when agreement between the experimental and simulated spectra is considered. In the case of 2.15 MeV (see Fig. 3(b)) and 2.2 MeV (see Fig. 4(a)), the experimental curves contain pronounced resonant peaks and a sharp decrease of intensity after the resonant peak, which closely follows the cross-section. On the other hand, the 2.25 MeV spectrum shows a gradual decrease of the intensity (see Fig. 2(b)). There might be several reasons to this. Firstly, this might indicate that particle channelling occurred deeper in the sample and the peak was shifted to the lower energy side. Additionally, this effect might be due to a digitization error; however, such disagreements with the experimental curves would be observed in other spectra digitized from the same reference and they are not observed. Finally, the low energy resonant peak might shift to lower energies due to the higher than described detector energy resolution or the influence of the detector dead layer, which was not taken into account during the simulations.

3.2. RBS from SiC sample

The proton induced backscattering spectra, obtained in the random orientation of SiC, were collected for proton energies of 1.5 and 1.7 MeV. The simulated and experimental spectra agree very well (see Fig. 5). In the case of 1.5 MeV, the experimental and simulated spectra match almost perfectly with the exception of a bump of intensity of the experimental curve at the 0.9–1.0 MeV energy and a slightly higher intensity at the 1.05–1.2 MeV region. The spectrum does not contain any resonance peaks and accommodates two clearly distinguishable bands that correspond to backscattering from Si (higher energy peaks) and C atoms. In the case of 1.7 MeV, the simulated and experimental spectra agree well, however, the intensity of the carbon resonant peak (at ~1.2 MeV) and silicon resonant peak (at ~1.4 MeV) is higher for the experimental spectrum, when compared to the simulated one. On the other hand, the energy positions and widths of the peaks, as well as the combined plateau region (0.4–1.1 MeV), are simulated well and a good match of the spectra is obtained.

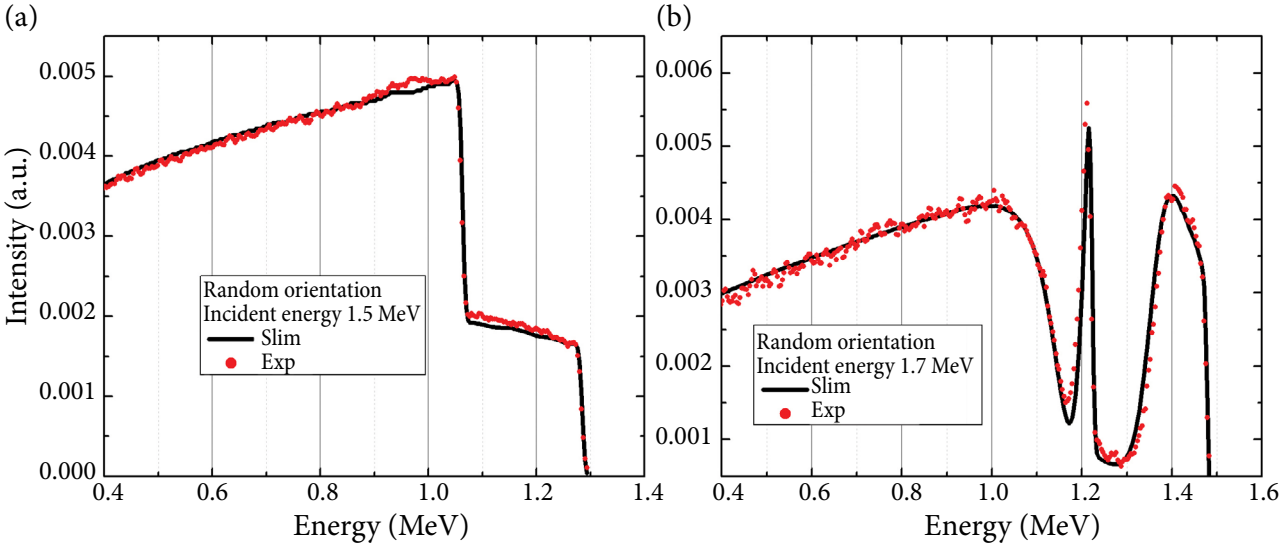

Fig. 5. Experimental and simulated backscattering spectra induced by 1.5 MeV (a) and 1.7 MeV (b) protons incident on the crystalline SiC sample under random orientation conditions. Experimental data digitized from Ref. [22].

3.3. RBS from SiO_2 sample

The comparison of the simulated and experimental backscattering spectra from a SiO_2 sample was performed for 1.6–1.8 MeV protons at a backscattering angle of 170°. The simulated spectra match the experimental spectra, obtained in the random orientation, almost perfectly (see Fig. 6). The energy positions of silicon (higher energy side) and oxygen bands are simulated correctly and the intensity of the simulated spectra agrees well with that of the experimental spectra. One key difference observed for 1.8 MeV protons is the higher intensity of the 1.2–1.4 MeV peak, which contains backscattering from both silicon and oxygen atoms.

For this particular sample a comparison was made between the experimental and simulated backscattering spectra, obtained in channelling conditions. The GEANT4 particle channelling model was previously modified, validated against the experimental data and proved to correctly evaluate the energy loss of channelled particles [24]. The model of the simulation of channelled particle backscattering spectra is still in a testing stage and will be described in the upcoming publication. This work only shows a preview of the capabilities of the model under development.

The proton particle beam was incident along the (0001) or optical axis (*c* axis) of crystalline SiO_2, while the simulated beam divergence was kept at 0.05–0.06° and proton energy in a range of 1.6–1.8 MeV. The match between the experimental and the simulated spectra is very good, especially in the case of 1.6 MeV (see Fig. 7(a)). One thing contrary to the amorphous case is that the bands corresponding to the backscattering from silicon and oxygen atoms are difficult to distinguish, specifically in the case of 1.6 MeV protons. For the spectra obtained in channelling conditions the maximum intensity of the spectra is shifted to lower energies. This is due to the backscattering occurring in deeper layers of the sample and the outgoing particle having to travel a larger distance when compared to an amorphous sample. The simulated 1.8 MeV proton induced backscattering spectrum is also in good agreement with the experimental spectrum, except for the energy region after the resonant peak (1.0–1.25 MeV). There are several reasons for this. First of all, virgin perfect single crystals were simulated, whereas the experimental crystals most likely contain a certain level of defects. Secondly, the simulated random orientation spectrum of 1.8 MeV protons shows a higher intensity of the resonant peak when compared to the experimental peak, thus the higher channelling geometry intensity may also be expected. This might occur due to the deviations of resonant peak cross-sections between the experimental and the theoretical values, or due to the slightly different conditions of the experiment (uncertainty of energy, angle, detector dead layer, etc.). Finally, the channelling model is still in development and might need some tweaking.

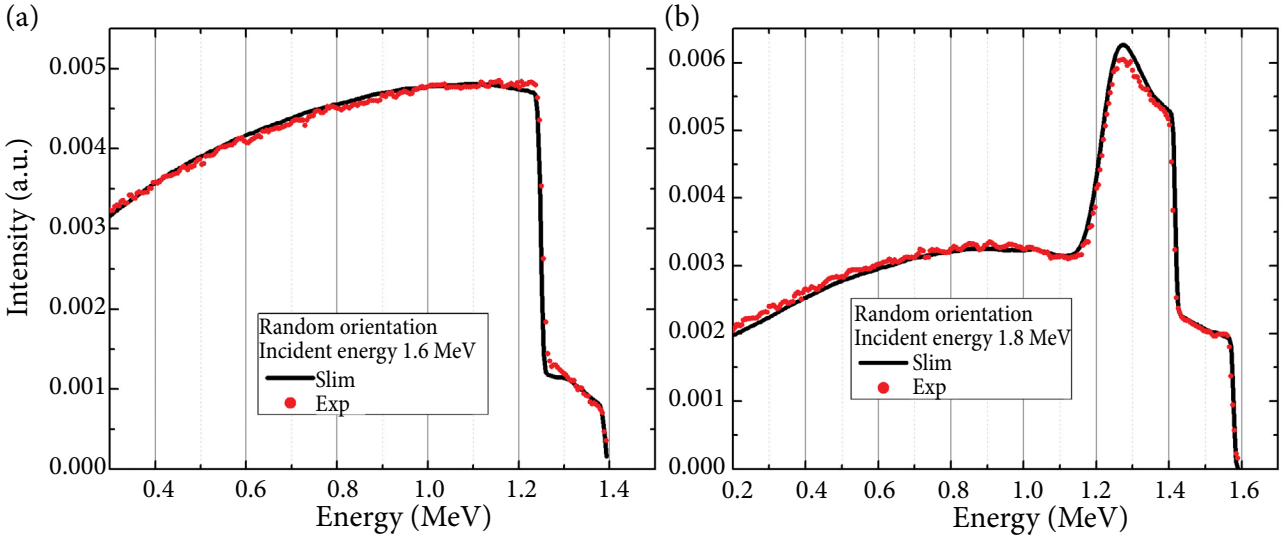

Fig. 6. Experimental and simulated backscattering spectra induced 1.6 MeV (a) and 1.8 MeV (b) protons incident on the crystalline SiO_2 sample under random orientation conditions. Experimental data digitized from Ref. [23].

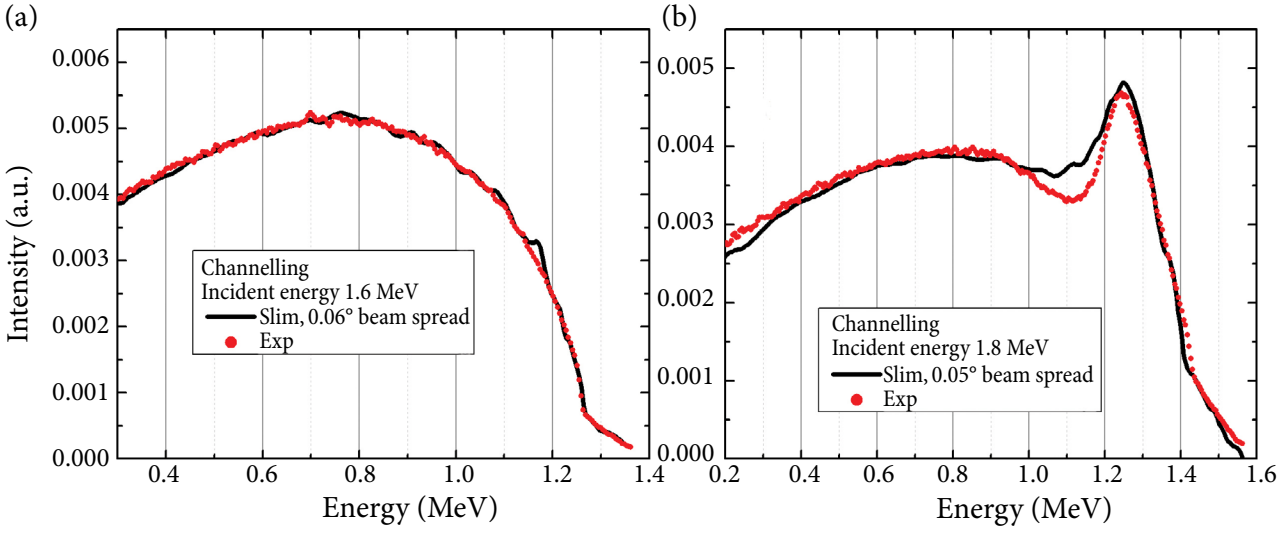

Fig. 7. Experimental and simulated backscattering spectra induced by 1.6 MeV (a) and 1.8 MeV (b) protons incident on the crystalline SiO_2 sample under particle channelling conditions. Experimental data digitized from Ref. [23].

Overall, both the channelling and random orientation spectra for silicon based samples are simulated with good agreement to the experimental spectra, and the GEANT4 RBS model is a great tool for the simulation and interpretation of proton backscattering spectra.

4. Summary and conclusions

This work presents the results of proton induced backscattering spectra simulations and comparisons with the experimental spectra in virgin silicon, silicon dioxide and silicon carbide single crystals, obtained in the random orientation conditions. The simulations were performed with a previously developed and described GEANT4 RBS model for amorphous materials. The comparison with the experimental spectra has shown that the model is able to accurately simulate the proton backscattering spectra in the energy interval 1.0–2.3 MeV for the random orientation conditions. The major mismatches between the simulated and experimental spectra occur for the resonant peaks, while the regions corresponding to backscattering from the sample surface are simulated very well. The mismatch in the resonant regions might be attributed to the limit of RTR cross-section accuracy or a slight mismatch of the incident energy, which would significantly influence the shape of the resonant curve as the resonant cross-sections are very energy-dependent. Overall, the match between the experimental and simulated spectra obtained in the random orientation conditions is within the expectations while the development of the model for better agreement is underway.

The work presented here also includes a preview of the simulations of backscattering spectra in the particle channelling conditions. The comparison between the experimental and simulated spectra, induced by the 1.6–1.8 MeV protons incident along the (1000) axis of a SiO_2 virgin single crystal, shows a good agreement with the mismatch of the spectra associated to the limits of the resonant cross-section database as well as the particle channelling process. Details of the simulation as well as the description of the newly developed model will be presented in the upcoming publications.

References

[1] A.O. Juma, Stoichiometry and local bond configuration of In_2S_3:Cl thin films by Rutherford backscattering spectrometry, Nucl. Instrum. Methods Phys. Res. B **385**, 84–88 (2016), https://doi.org/10.1016/j.nimb.2016.09.005

[2] N. Nishikata, K. Kushida, T. Nishimura, T. Mishima, K. Kuriyama, and T. Nakamura, Evaluation of lattice displacement in Mg – Implanted GaN by Rutherford backscattering spectroscopy, Nucl. Instrum. Methods Phys. Res. B

409, 302–304 (2017), https://doi.org/10.1016/j.nimb.2017.03.125

[3] S. Magalhães, N.P. Barradas, E. Alves, I.M. Watson, and K. Lorenz, High precision determination of the InN content of $Al_{1-x}In_xN$ thin films by Rutherford backscattering spectrometry, Nucl. Instrum. Methods Phys. Res. B **273**, 105–108 (2012), https://doi.org/10.1016/j.nimb.2011.07.051

[4] B. Lukasc, Correction of the limited energy resolution in RBS spectra, Phys. Status Solidi **64**(2), 533–538 (1981), https://doi.org/10.1002/pssa.2210640217

[5] P. Bauer, E. Steinbauer, and J.P. Biersack, The width of an RBS spectrum: influence of plural and multiple scattering, Nucl. Instrum. Methods Phys. Res. B **64**(1–4), 711–715 (1992), https://doi.org/10.1016/0168-583X(92)95563-7

[6] J.F. Ziegler, RBS/ERD simulation problems: Stopping powers, nuclear reactions and detector resolution, Nucl. Instrum. Methods Phys. Res. B **136–138**, 141–146 (1998), https://doi.org/10.1016/S0168-583X(97)00664-2

[7] E. Kótai, Computer methods for analysis and simulation of RBS and ERDA spectra, Nucl. Instrum. Methods Phys. Res. B **85**(1–4), 588–596 (1994), https:///doi.org/10.1016/0168-583X(94)95888-2

[8] F. Schiettekatte, Fast Monte Carlo for ion beam analysis simulations, Nucl. Instrum. Methods Phys. Res. B **266**(8), 1880–1885 (2008), https://doi.org/10.1016/j.nimb.2007.11.075

[9] E. Szilágyi and F. Pászti, Theoretical calculation of the depth resolution of IBA methods, Nucl. Instrum. Methods Phys. Res. B **85**(1–4), 616–620 (1994), https://doi.org/10.1016/0168-583X(94)95893-9

[10] M. Mayer, SIMNRA, a simulation program for the analysis of NRA, RBS and ERDA, AIP Conf. Proc. **475**(1), 541–544 (1999), https://doi.org/10.1063/1.59188

[11] C. Jeynes, N.P. Barradas, P.K. Marriott, G. Boudreault, M. Jenkin, E. Wendler, and R.P. Webb, Elemental thin film depth profiles by ion beam analysis using simulated annealing – a new tool, J. Phys. D **36**(7), R97 (2003), https://doi.org/10.1088/0022-3727/36/7/201

[12] D. Lingis, M. Gaspariūnas, V. Kovalevskij, A. Plukis, and V. Remeikis, A model to simulate large angle Rutherford backscattering spectra in GEANT4, Comput. Phys. Commun. **271**, 108187 (2022), https://doi.org/10.1016/J.CPC.2021.108187

[13] S. Agostinelli, J. Allison, K. Amako, J. Apostolakis, H. Araujo, P. Arce, M. Asai, D. Axen, S. Banerjee, G. Barr, and F. Behner, GEANT4 – a simulation toolkit, Nucl. Instrum. Methods Phys. Res. A **506**(3), 250–303 (2003), https://doi.org/10.1016/S0168-9002(03)01368-8

[14] H.R. Verma, *Atomic and Nuclear Analytical Methods*, Vol. 1 (Springer Berlin Heidelberg, Berlin, 2007) pp. 91–141.

[15] M. Kokkoris, S. Dede, K. Kantre, A. Lagoyannis, E. Ntemou, V. Paneta, K. Preketes-Sigalas, G. Provatas, R. Vlastou, I. Bogdanović-Radović, Z. Siketić, and N. Obajdin, Benchmarking the evaluated proton differential cross sections suitable for the EBS analysis of ^{nat}Si and ^{16}O, Nucl. Instrum. Methods Phys. Res. B **405**, 50–60 (2017), https://doi.org/10.1016/j.nimb.2017.05.021

[16] H.H. Andersen, F. Besenbacher, P. Loftager, and W. Möller, Large-angle scattering of light ions in the weakly screened Rutherford region, Phys. Rev. A **21**(6), 1891–1901 (1980), https://doi.org/10.1103/PhysRevA.21.1891

[17] A.F. Gurbich, SigmaCalc recent development and present status of the evaluated cross-sections for IBA, Nucl. Instrum. Methods Phys. Res. B **371**, 27–32 (2016), https://doi.org/10.1016/j.nimb.2015.09.035

[18] R. Ankit, *WebPlotDigitizer* (Pacifica, California, USA, 2022), https://automeris.io/WebPlotDigitizer/index.html

[19] X.A. Aslanoglou, P.A. Assimakopoulos, M. Kokkoris, and E. Kossionides, Simulations of channeling spectra in the system p+^{28}Si, Nucl. Instrum. Methods Phys. Res. B **140**(3–4), 294–302 (1998), https://doi.org/10.1016/S0168-583X(98)00112-8

[20] M. Kokkoris, G. Perdikakis, S. Kossionides, S. Petrovic, and E. Simoen, On the dechanneling of protons in Si [110], Eur. Phys. J. B **34**(3), 257–263 (2003), https://doi.org/10.1140/EPJB/E2003-00219-Y

[21] X.A. Aslanoglou, A. Karydas, M. Kokkoris, E. Kossionides, Th. Paradellis, G. Souliotis, and R. Vlastou, Simulations and comparisons of channeling spectra in the p+^{28}Si system in the backscattering geometry, Nucl. Instrum. Methods Phys. Res. B, **161–163**, 524–527 (2000), https://doi.org/10.1016/S0168-583X(99)00781-8

[22] M. Kokkoris, S. Kossionides, R. Vlastou, X.A. Aslanoglou, R. Grötzschel, B. Nsouli, A. Kuznetsov, S. Petrovic, and Th. Paradellis, Determination of parameters for channeling of protons in SiC polytype crystals in the backscattering geometry, Nucl. Instrum. Methods Phys. Res. B **184**(3), 319–326 (2001), https://doi.org/10.1016/S0168-583X(01)00727-3

[23] M. Kokkoris, R. Vlastou, X.A. Aslanoglou, E. Kossionides, R. Grötzschel, and T. Paradellis, Determination of the stopping power of channeled protons in SiO_2 in the backscattering geometry, Nucl. Instrum. Methods Phys. Res. B **173(**4), 411–416 (2001), https://doi.org/10.1016/S0168-583X(00)00432-8

[24] D. Lingis, M. Gaspariūnas, A. Plukis, and V. Remeikis, Improvements and validation of particle channeling model in GEANT4, Nucl. Instrum. Methods Phys. Res. B **525**, 1–12 (2022), https://doi.org/10.1016/J.NIMB.2022.05.007

PROTONŲ ATGALINĖS SKLAIDOS SPEKTRŲ SKAITINIS MODELIAVIMAS GEANT4 PROGRAMINIU PAKETU

D. Lingis, M. Gaspariūnas, V. Kovalevskij, A. Plukis, V. Remeikis

Fizinių ir technologijos mokslų centras, Vilnius, Lietuva

Santrauka

Rezerfordo atgalinės sklaidos spektroskopija (angl. *Rutherford Backscattering Spectroscopy*, *RBS*) yra metodika, plačiai naudojama bandinių sudėties, kristalinių gardelių pažaidų ir priemaišų profiliavimo analizėse. Metodika paremta į bandinį krintančių jonų elastine sklaida ir atgal išsklaidytų dalelių energinio spektro registravimu detektoriumi. Tačiau atgalinės sklaidos spektrų interpretavimas sukelia sunkumų dėl persiklojančių smailių, atitinkančių sklaidą nuo skirtingų atomų, ir sklaidos geometrijos, energijos nuostolių bei detektoriaus atsako neapibrėžčių. Siekiant palengvinti spektrų interpretavimo procesą, buvo sukurtas atviro kodo skaitinio modeliavimo pavyzdys, paremtas universaliu GEANT4 skaitinio modeliavimo programiniu paketu. Atviro kodo modelio lankstumas leidžia naudotojams pritaikyti modelį savo tikslams – nuo galimybės naudoti įvairias dalelių stabdomųjų gebų ir reakcijų skerspjūvių bibliotekas bei modifikuoti fizikinius procesus iki galimybės sekti dalelių parametrus. Šio darbo metu pristatyti eksperimentinių ir skaitiškai modeliuotų atgalinės sklaidos spektrų palyginimo rezultatai, gauti naudojant 1–2,5 MeV energijos protonų pluoštelį kristalinio silicio, silicio karbido ir silicio dioksido bandiniuose atsitiktinės orientacijos geometrijoje, kuri praktiškai atitinka amorfinių medžiagų atvejį. Pateikti rezultatai rodo, kad modelis geba tiksliai skaitiškai atkartoti atgalinės sklaidos spektrus nuo amorfinių ir kristalinių medžiagų. Nors ideali atitiktis eksperimentiniams spektrams nebuvo gauta visais atvejais, bendras spektrų atitikimas rodo, kad modelį galima toliau tobulinti ir naudoti RBS metodikoje.